

# Optimizing Superconductivity in Sr<sub>2</sub>RuO<sub>4</sub> Thin Films with Varying Cation Flux Ratio Grown by Molecular-Beam Epitaxy

Casey K. Kim<sup>1</sup>, Jinkwon Kim<sup>1</sup>, and Darrell G. Schlom<sup>1</sup>

<sup>1</sup> *Department of Materials Science and Engineering, Cornell University, Ithaca, NY 14853*

## Abstract

Epitaxial samples of Sr<sub>2</sub>RuO<sub>4</sub> were grown on NdGaO<sub>3</sub> (110) substrate by molecular-beam epitaxy (MBE) to optimize its superconductivity. Challenges in growing superconducting Sr<sub>2</sub>RuO<sub>4</sub> include intergrowth of Ruddlesden-Popper perovskite phases and the possibility of ruthenium deficiency in the sample. In this study, we investigate the effects of varying the cation flux ratio on the film crystallinity and transport properties. Notably, we observed superconducting transition temperature,  $T_c^{mid}$ , as high as 2.05 K in our experimental results, which is the highest value ever reported.

## Introduction

Superconductivity of strontium ruthenate Sr<sub>2</sub>RuO<sub>4</sub> was first discovered in 1994 by Y. Maeno and his collaborators [1]. Its potential as a *p*-wave superconductor and structural similarities to high temperature superconducting cuprates have garnered interests among researchers [2, 3]. Numerous efforts have been made to study superconductivity in Sr<sub>2</sub>RuO<sub>4</sub>, and we aim to further optimize the superconducting temperature of Sr<sub>2</sub>RuO<sub>4</sub> in this project.

The growth of superconducting Sr<sub>2</sub>RuO<sub>4</sub> thin films poses several challenges, primarily due to the material's sensitivity to disorder [4, 5]. The parent phase of Sr<sub>2</sub>RuO<sub>4</sub> is Ruddlesden-Popper perovskite, expressed as A<sub>n+1</sub>B<sub>n</sub>O<sub>3n+1</sub>, where A is a rare earth element, and B is a transition metal element. When growing strontium ruthenates, there is a possibility of observing intergrowth of these phases. However, by carefully choosing growth condition by referring to thermodynamics of MBE (TOMBE) diagram, this intergrowth can be prevented [6]. It is crucial to avoid such intergrowth, as the presence of impurity phases in the sample may suppress superconductivity [4]. In addition, ruthenium vacancy can also hinder the superconductivity in Sr<sub>2</sub>RuO<sub>4</sub> [5].

To optimize the superconductivity in Sr<sub>2</sub>RuO<sub>4</sub>, we investigate the choice of substrates and vary the flux ratio between strontium and ruthenium atoms. Following from a study that exhibits enhanced superconductivity of Sr<sub>2</sub>RuO<sub>4</sub> in bulk under uniaxial stress, we will compare two commonly used substrates for growing epitaxial Sr<sub>2</sub>RuO<sub>4</sub>: NdGaO<sub>3</sub> (110) and (LaAlO<sub>3</sub>)<sub>0.3</sub>(Sr<sub>2</sub>AlTaO<sub>6</sub>)<sub>0.7</sub> (LSAT) (001) [7]. Furthermore, we examine samples with 2Ru/Sr flux ratios of 1.7, 1.9, and 2.1 to study the effect of supplying excess ruthenium on the characteristics of the film.

## Methods

All Sr<sub>2</sub>RuO<sub>4</sub> samples were grown by Veeco Gen10 oxide MBE system for this project. The elemental flux for strontium was estimated using Quartz Crystal Microbalance (QCM). By multiplying the strontium flux by empirical tooling factor, ruthenium flux was then calibrated with QCM to achieve the desired 2Ru/Sr flux ratios of 1.7, 1.9, and 2.1. The e-beam evaporated ruthenium source's Electron Impact Emission Spectroscopy (EIES) value was recorded at the desired QCM flux value. Throughout the growth, it is important to monitor EIES value and adjust the current of the e-beam evaporator accordingly to maintain a constant ruthenium flux.

All samples were grown on  $\text{NdGaO}_3$  (110) substrates, as mentioned earlier. Lattice misfit strain between  $\text{Sr}_2\text{RuO}_4$  and  $\text{NdGaO}_3$  (110) is  $-0.39\%$  along [001] in-plane direction and  $-0.16\%$  along  $[1\bar{1}0]$  in-plane direction [6, 8, 9]. In contrast, the lattice misfit strain between  $\text{Sr}_2\text{RuO}_4$  and LSAT (001) is  $-0.08\%$  [10]. Due to the larger compressive epitaxial strain,  $\text{NdGaO}_3$  (110) was chosen over LSAT (001) in our experiment with the goal of enhancing superconductivity in our films [7].

The growth condition of the film was set by thermodynamics of MBE (TOMBE) diagram [6]. The same growth conditions were applied to all the films, with a substrate temperature ( $T_{\text{pyrometer}}$ ) of  $940^\circ\text{C}$  and oxygen pressure of  $6 \times 10^{-7}$  Torr with distilled ozone.

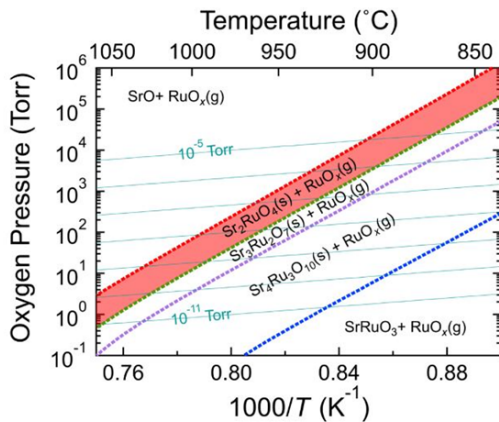


Figure 1. TOMBE diagram for adsorption-controlled growth window for  $\text{Sr}_2\text{RuO}_4$  [6, Fig. 1]

After growth, the films were characterized by  $\text{Cu-K}\alpha 1$  X-ray diffraction (XRD) to confirm the phase purity and crystal structure of the film. In addition, rocking curves were collected to further assess the crystalline quality of the samples. Then, the surface topology was imaged by Atomic Force Microscopy (AFM). Transport properties were measured with a Quantum Design PPMS He-3 system. The sample's resistivity was measured against temperature using four-point probe method, while magnetoresistance was recorded by monitoring the change in resistivity with externally applied magnetic field at  $450\text{ mK}$ .

## Results and Discussion

To investigate the crystallinity and phase-purity of the films, XRD was measured for each sample as presented in Figure 2. For the sample with a  $2\text{Ru/Sr}$  flux ratio of 1.7, Laue oscillations were observed, indicating a high-quality film that is well aligned crystallographically. However, Laue oscillations were not observed in the samples grown with larger  $2\text{Ru/Sr}$  flux ratios. Additionally, (006) peak of  $\text{Sr}_2\text{RuO}_4$  is observed at  $2\theta$  value of  $42.44$  degrees, as shown in Figure 2(d)-(f). By extracting the peak location of the film, we calculated the out-of-plane spacing of the film using Bragg's law, obtaining a value of  $c = 12.769\text{ \AA}$ . This is slightly greater than the  $c$ -axis lattice parameter of the single-crystal  $\text{Sr}_2\text{RuO}_4$  ( $c = 12.746\text{ \AA}$ ), confirming the presence of compressive epitaxial strain on the film [6]. Furthermore, no film peaks other than  $\text{Sr}_2\text{RuO}_4$  were observed any of the samples, indicating that the films are phase-pure with no intergrowth of unwanted Ruddlesden-Popper perovskite phases.

Similarly, the crystallinity and quality of the film were assessed by rocking curves measured at the main peak of the sample. Figure 3(a) presents a combined rocking curves of the three films grown with different flux ratios, and their full width at half maximum (FWHM) values are tabulated in Figure 3(b). The film grown with  $2\text{Ru/Sr}$  flux ratio of 1.7 demonstrated the sharpest rocking curve with FWHM value of  $0.02^\circ$ . This confirms the high crystallinity of the sample, as shown by the presence of Laue oscillations in Figure 2. In comparison, films grown with  $2\text{Ru/Sr}$  flux ratios of 1.9 and 2.1 showed lesser crystallinity, as indicated by their larger FWHM values of  $0.10^\circ$ .

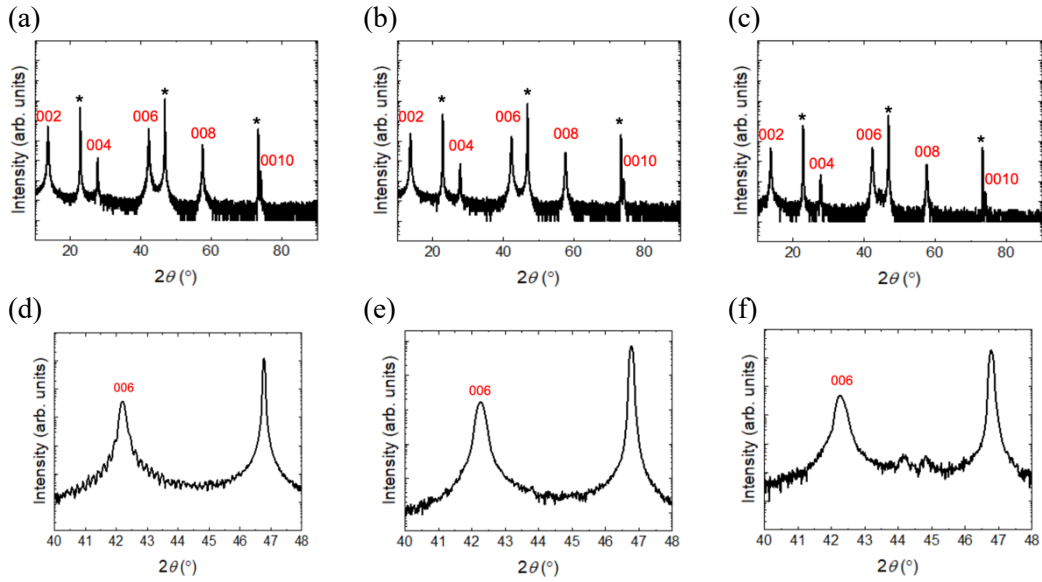


Figure 2. (a)-(c) exhibit X-ray diffraction data of  $\text{Sr}_2\text{RuO}_4$  films grown on  $\text{NdGaO}_3$  (110) substrate for 2Ru/Sr flux ratios of 1.7, 1.9, and 2.1, respectively. All the peaks are indexed to either the film or the substrate peaks (asterisks).  $\theta$ - $2\theta$  scans of  $\text{Sr}_2\text{RuO}_4$  films exhibit phase-pure growth. (d)-(f) show the  $\theta$ - $2\theta$  scans around the main peak of samples (a)-(c), respectively.

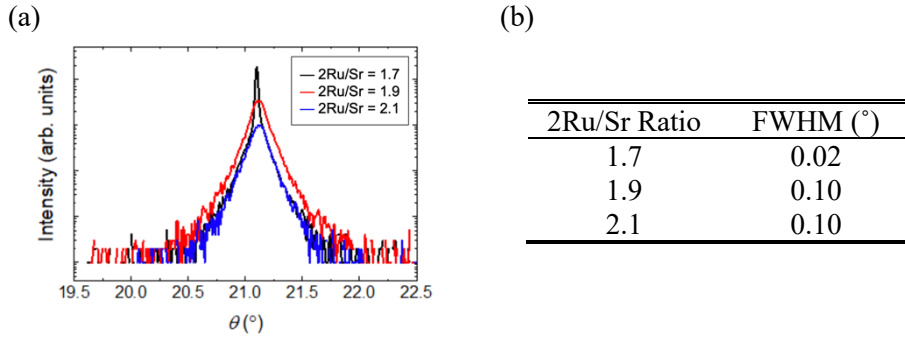


Figure 3. (a) illustrates rocking curve measurements of  $\text{Sr}_2\text{RuO}_4$  films grown on  $\text{NdGaO}_3$  (110) substrate for 2Ru/Sr flux ratios of 1.7, 1.9, and 2.1. Black line shows dataset for flux ratio of 1.7, red line shows dataset for flux ratio of 1.9, and blue line shows dataset for flux ratio of 2.1. The same color coding will be used in the remaining report. (b) shows tabulated data of the full width at half maximum values of the rocking curve measurements presented in (a).

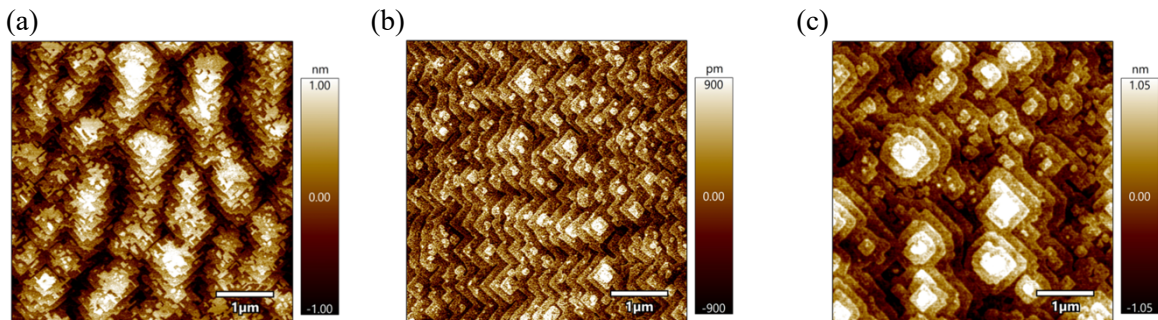


Figure 4. (a), (b), and (c) show AFM images for 2Ru/Sr flux ratio of 1.7, 1.9, and 2.1, respectively.

Figure 4 exhibits surface topology of the films measured by AFM. The root mean surface roughness was measured to be 0.46 nm, 0.36 nm, and 0.42 nm for flux ratios of 1.7, 1.9, and 2.1, respectively. Despite the high crystallinity of the sample with a flux ratio of 1.7, its surface roughness was greater than the other two samples.

The resistivity measurement as a function of temperature of all films revealed superconductivity, as shown in Figure 5. Interestingly, we observed an increasing superconducting critical temperature with increasing ruthenium flux. This observation aligns with the sensitivity to ruthenium vacancies of  $\text{Sr}_2\text{RuO}_4$  thin films, as previously reported [5]. By supplying surplus ruthenium flux to the film, the concentration of ruthenium vacancies decreased, leading to an enhancement of superconductivity. Notably, we achieved a critical temperature,  $T_c^{mid}$ , as high as 2.05 K, the highest critical temperature reported for  $\text{Sr}_2\text{RuO}_4$  thin films in the literature. Moreover, the residual resistivity ratio (RRR), calculated by dividing the resistivity of the sample at 300 K by that at 2.5 K, showed improvements with increased ruthenium flux. This increase in RRR corresponds to a reduction in defects, such as ruthenium vacancies, within the sample.

To gain further insights into transport phenomena, we measured the magnetoresistance of the samples, as illustrated in Figure 6. This allowed us to observe the magnitude of critical magnetic field that the films can withstand while maintaining their superconductivity. The sample grown with 2Ru/Sr flux ratio of 1.7 exhibited a critical magnetic field of  $\sim 3$  kOe, while the other two samples showed a critical magnetic field of  $\sim 4$  kOe. With increased in ruthenium content in the crystal, the films were able to maintain its superconductivity under stronger magnetic fields, further highlighting the significance of ruthenium vacancies in  $\text{Sr}_2\text{RuO}_4$  and their impact on its superconductivity.

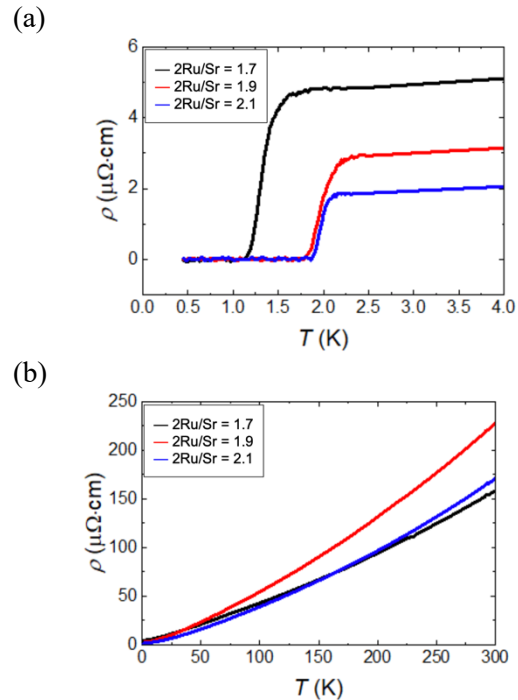


Figure 5. (a) resistivity vs. temperature of  $\text{Sr}_2\text{RuO}_4$  films grown on  $\text{NdGaO}_3$  (110) substrate for 2Ru/Sr flux ratios of 1.7, 1.9, and 2.1. Critical temperature measured at 50% of the superconducting transition,  $T_c^{mid}$ , is 1.30 K for the film grown with 2Ru/Sr flux ratio of 1.7, 1.95 K for the flux ratio of 1.9, and 2.05 K for the flux ratio of 2.1. (b) The RRR is 33 for the film grown with 2Ru/Sr flux ratio of 1.7, 79 for the flux ratio of 1.9, and 93 for the flux ratio of 2.1.

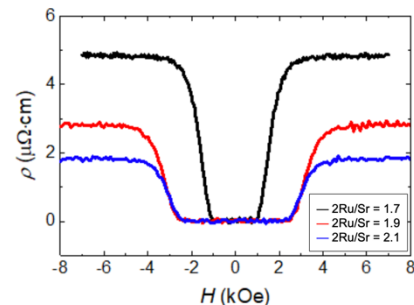


Figure 6. Magnetoresistance measurements of  $\text{Sr}_2\text{RuO}_4$  films grown on  $\text{NdGaO}_3$  (110) substrate for 2Ru/Sr flux ratios of 1.7, 1.9, and 2.1. The sample grown with the flux ratio of 1.7 roughly has critical magnetic field  $H_{c2}^\perp$  of 3 kOe, and the other two samples have critical magnetic field  $H_{c2}^\perp$  of about 4 kOe.

## Conclusion and Future Work

In summary, we successfully grew  $\text{Sr}_2\text{RuO}_4$  thin films with enhanced superconductivity by varying ruthenium flux. Although Laue oscillations from XRD and rocking curves suggested that ruthenium deficient sample holds higher crystal quality, the transport properties of the sample showed improvement with increasing ruthenium content. Moving forward, we plan to investigate the magnetic structure of the  $\text{Sr}_2\text{RuO}_4$  by mu ion scattering experiments with our optimized growth condition of 2Ru/Sr flux ratio of 2.1.

## Acknowledgements

I thank my mentor Dr. Jinkwon Kim and PI Professor Darrell G. Schlom for their support and guidance in this project. This research was funded by the National Science Foundation (NSF) Platform for the Accelerated Realization, Analysis, and Discovery of Interface Materials (PARADIM) under Cooperative Agreement No. DMR-2039380 as well as the NSF REU Site: Summer Research Program at PARADIM under Cooperative Assignment No. DMR-2150446.

## References

- [1] Y. Maeno et al., *Nature* **372**, 532-534 (1994)
- [2] K. D. Nelson et al., *Science* **306**, 1141-1154 (2004)
- [3] Y. Maeno et al., *Physics Today*. **54**, 42-47 (2001)
- [4] A. P. Mackenzie et al., *Phys. Rev. Lett.* **80**, 161 (1998)
- [5] G. Kim et al., *Phys. Rev. Mater.* **3**, 94802 (2019)
- [6] H. Nair et al., *APL Materials* **6**, 101108 (2018)
- [7] A. Steppke et al., *Science* **355**, eaaf9398 (2017)
- [8] M. Schmidbauer et al., *Acta Cryst.* **B68**, 8 (2012)
- [9] L. Walz and F. Lichtenberg, *Acta Cryst.* **C49**, 1268-1270 (1993)
- [10] C.M.P. Garcia et al., *Commun. Mater.* **1**, 23 (2020)